Journal of Materials Chemistry B

ROYAL SOCIETY OF CHEMISTRY

PAPER

View Article Online
View Journal | View Issue

Cite this: J. Mater. Chem. B, 2021, 9, 7205

Hyaluronic acid drives mesenchymal stromal cell-derived extracellular matrix assembly by promoting fibronectin fibrillogenesis†

Marisa Assunção, [ab] Chi Him Kendrick Yiu, [ab] Ho-Ying Wan, [ab] Dan Wang, [abcd] Dai Fei Elmer Ker, [abcd] Rocky S. Tuan [ab] and Anna Blocki *[abc]

Hyaluronic acid (HA)-based biomaterials have been demonstrated to promote wound healing and tissue regeneration, owing to the intrinsic and important role of HA in these processes. A deeper understanding of the biological functions of HA would enable better informed decisions on applications involving HA-based biomaterial design. HA and fibronectin are both major components of the provisional extracellular matrix (ECM) during wound healing and regeneration. Both biomacromolecules exhibit the same spatiotemporal distribution, with fibronectin possessing direct binding sites for HA. As HA is one of the first components present in the wound healing bed, we hypothesized that HA may be involved in the deposition, and subsequently fibrillogenesis, of fibronectin. This hypothesis was tested by exposing cultures of mesenchymal stromal cells (MSCs), which are thought to be involved in the early phase of wound healing, to high molecular weight HA (HMWHA). The results showed that treatment of human bone marrow derived MSCs (bmMSCs) with exogenous HMWHA increased fibronectin fibril formation during early ECM deposition. On the other hand, partial depletion of endogenous HA led to a drastic impairment of fibronectin fibril formation, despite detectable granular presence of fibronectin in the perinuclear region, comparable to observations made under the well-established ROCK inhibition-mediated impairment of fibronectin fibrillogenesis. These findings suggest the functional involvement of HA in effective fibronectin fibrillogenesis. The hypothesis was further supported by the co-alignment of fibronectin, HA and integrin α5 at sites of ongoing fibronectin fibrillogenesis, suggesting that HA might be directly involved in fibrillar adhesions. Given the essential function of fibronectin in ECM assembly and maturation, HA may play a major enabling role in initiating and propagating ECM deposition. Thus, HA, as a readily available biomaterial, presents practical advantages for *de novo* ECM-rich tissue formation in tissue engineering and regenerative medicine.

Received 9th February 2021,
Accepted 4th March 2021

DOI: 10.1039/d1tb00268f

rsc.li/materials-b

Introduction

HA is a key biomacromolecule of the ECM and is composed of repeating glucuronic acid and *N*-acetylglucosamine disaccharides $[-\beta(1,4)\text{-GlcUA-}\beta(1,3)\text{-GlcNAc}-]_n$. About 0.02% of a person's bodyweight can be attributed to HA, which is abundantly present in many tissues such as the skin. It has a fast turn-over rate (30% per day) and is upregulated during tissue remodelling.[1] Its cell- and histocompatibility, as well as intrinsic role in tissue development and repair[2] make HA a biopolymer of choice in a vast range of biomaterials designed to limit fibrosis, accelerate wound healing, and augment functional recovery.[3–7]

Missinato and colleagues showed that the difference between achieving regeneration *versus* scarring relied on the availability of HA in sufficient amounts throughout the wound healing process.[8] Biological processes, such as cellular proliferation, migration and differentiation, as well as inflammatory processes and the extent of fibrosis are influenced by HA as a function of its molecular weight (size) and the physiological context.[6] Upon tissue injury, HMWHA originating from blood, platelets and the surrounding damaged tissue is released into

[a] Institute for Tissue Engineering and Regenerative Medicine, The Chinese University of Hong Kong (CUHK), Shatin, Hong Kong SAR, China. E-mail: anna.blocki@cuhk.edu.hk
[b] School of Biomedical Sciences, CUHK, Shatin, Hong Kong SAR, China
[c] Department of Orthopaedics & Traumatology, Faculty of Medicine, CUHK, Shatin, Hong Kong SAR, China
[d] Key Laboratory for Regenerative Medicine, Ministry of Education, School of Biomedical Sciences, Faculty of Medicine, The Chinese University of Hong Kong, Shatin, Hong Kong SAR, China

† Electronic supplementary information (ESI) available: Fig. S1. See DOI: 10.1039/d1tb00268f

the injury site, where it contributes to the formation of the early provisional wound matrix.[9,10] Due to its hygroscopic nature, a desirable biophysical attribute for hydrogel biopolymer,[3] HA facilitates the formation of a porous network that is advantageous for diffusion of signalling molecules and the infiltration of inflammatory cells.[9,11] These inflammatory cells are regulated by HA, as it accumulates during the formation of the second order provisional matrix.[12,13] Contrary to its shorter chain homologs, HMWHA exhibits strong anti-inflammatory activity.[12,13] This characteristic highlights the potential of HMWHA-based biomaterials for the treatment of chronically inflamed clinical conditions.[14]

Concomitantly with HA, fibronectin is also an early ECM component to be deposited.[15–17] Its fibrillar assembly is necessary for other ECM components, such as fibrillin 1 and collagen type I to be deposited.[17–19] Fibronectin is incorporated into the ECM *via* cell-mediated fibrillogenesis, a multi-step, integrin-dependent process.[20,21] First, it is initiated by binding of soluble globular fibronectin molecules to integrin α5β1 receptors on the cell membrane. Subsequently, integrin receptors translocate bundles of actin filaments in a Rho-mediated manner towards the center of the cell.[21,22] The resulting cell-generated forces induce conformational changes in the fibronectin molecules, elongating them and exposing cryptic fibronectin–fibronectin binding sites.[20,23,24] Aggregation of α5β1 integrins at pericentral location allows for intermolecular interaction of elongated fibronectin molecules, leading to the assembly of fibronectin fibrils.[25,26]

Interestingly, the N-terminal side of fibronectin was identified as a binding side for HA,[27,28] where a large amount of positively charged amino acids (mainly lysine) reside.[29] During wound healing and regeneration, HA and fibronectin follow the same spatial and temporal distribution in the reorganizing tissue, with HA being present during the stage of fibronectin deposition.[30–32] Indeed, the use of exogenous HA as a solution or gel was shown to promote fibronectin deposition *in vitro*[33,34] and *in vivo*,[35] albeit controversial reports to this finding exist.[36,37] Nevertheless, the role of fibronectin–HA interactions and the relevance of their co-presence in wound healing remain unknown. Since HA is one of the first ECM components present during tissue remodelling, we hypothesized that HA may also be involved in the process of fibronectin fibrillogenesis and therefore in the formation of the second order provisional matrix.

The clarification of such a fundamental function of HA during wound healing and regeneration would provide a strong rationale for the adoption of HA as a promising biomacromolecule in application-driven biomaterial design, for the purpose of promoting ECM deposition and thus *de novo* tissue formation *in vitro* and *in vivo*.

To test this hypothesis, cultures of mesenchymal stromal cells (MSCs) were exposed to a range of HMWHA concentrations and the cell-mediated assembly of the provisional matrix *in vitro* was investigated. MSCs, which are excellent ECM producers, were studied, as they are one of the recruited cell type to promote wound healing.[38,39] Human bone marrow-derived MSCs (bmMSCs), one of the major ECM-producing stromal cell types utilized in regenerative therapies,[15,40] were used to study ECM assembly in response to HA.

Results

Exogenously added HA increased deposition of fibrillar fibronectin

Human bmMSCs were cultured in the presence of HA (M_r = 1.6 MDa) at concentrations ranging from 0–500 μg ml^{-1} for 2 days. Higher concentrations (1000 μg ml^{-1}) visibly affected the viscosity of the HA solution and were thus excluded from the experiment. The cultured cells were then immunostained for fibronectin and the respective surface area coverage was quantified and normalized to the number of cells (based on DAPI-positive counts) in the respective imaged area (imaged area = 15% of total well). Supplementation with highest HA concentration (500 μg ml^{-1}) led to significantly increased fibronectin deposition (Fig. 1A and B). It should be noted that although cells used here were cultured in medium with low serum concentration (0.5%), cellular fibronectin assembly could still be masked by non-specific adsorption of serum-derived fibronectin. As the appropriate incorporation of fibronectin into the ECM involves a cell-mediated fibrillogenesis process,[21] we investigated the effect of varying HA concentrations on the deposition of fibrillar fibronectin. We first removed non-fibrillar, globular fibronectin using existing protocols,[41] based on the reported solubility of fibronectin in the non-ionic detergent, DOC.[41] The remaining fibrillar fibronectin in the cell layer was quantified. As the ECM was relatively unstable after only 2 days in culture, the partial cell lysis and ECM removal upon DOC treatment could result in variable amounts of deposited fibronectin. Nevertheless, a HA concentration-dependent increase in fibronectin fibril deposition was observed, reaching significance at concentrations of 50 μg ml^{-1} and above (Fig. 1A and B). An independent cell proliferation assay demonstrated no cell proliferation effect of HA at this early timepoint (Fig. 1C), suggesting that HA-mediated enhancement of fibrillar fibronectin deposition was unrelated to an increase in cell number. To investigate if supplementation of exogenous HA would affect the deposition of other major ECM components, we also stained the respective cell layers for collagen type I at day 2 and 6. At day 2 only very limited amounts of collagen type I were detected. By day 6 a substantial amount of collagen type I was deposited, although no significant differences in the overall amount were observed upon HA treatment at various HA concentrations and the control (Fig. 1D and E). We and others have previously shown that most marked differences in collagen type I deposition can be observed by day 6 or 7, whereas at later time points an equal plateau in collagen type I deposition is often approached in all conditions.[33,42,43] These data show that exogenous HA dose-dependently increased fibrillar fibronectin assembly.

Inhibition of fibronectin fibrillogenesis did not affect HA presence or distribution

In accordance to previous reports stating that HA directly interacted with fibronectin,[44] we stained endogenous HA using hyaluronic acid binding protein (HABP), and investigated its cellular distribution in relation to fibronectin by confocal

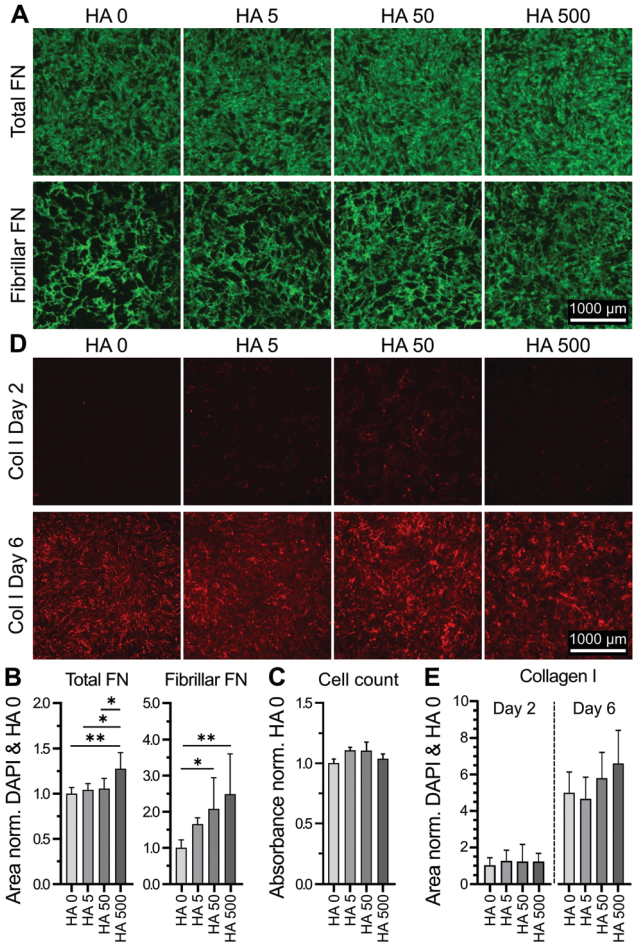

Fig. 1 Exogenously added HA increased deposition of fibrillar fibronectin (FN) in the cell layer. Cultures of human bmMSCs were incubated for 2 days with [HA] 0–500 µg ml^{-1}. (A) Representative images of FN before (total FN) and after deoxycholate (DOC) wash (fibrillar FN) visualized by immunocytochemistry. (B) Total FN was quantified as FN area coverage normalized to cell count (DAPI count of the same imaged area). Both total and fibrillar FN were normalized to respective controls (HA 0). A HA concentration-dependent effect on fibrillar FN deposition was observed. (C) Cell proliferation assay (CCK-8) determined cell number in day 2 cultures. Absorbance values were normalized to HA 0 control and show no statistical differences in between the various conditions. (D) Representative images of immunostained collagen type I (col I) in bmMSC layers at day 2 and 6. (E) Quantification of deposited col I (area coverage) normalized to DAPI count and HA 0. Collagen I was substantially deposited by day 6 of culture, although deposited amounts were not affected by the various concentrations of HMWHA. *$p < 0.05$, **$p < 0.001$. Scale bar = 1000 µm. n = 10 biological replicates.

microscopy at day 2 of culture. As shown in Fig. 2, the depicted cell showed a characteristic pattern of fibronectin with distinct fibers extending from a pericentral area to the outskirts of the cell and pre-fibrillar fibronectin (granular fibronectin staining aligned in the direction of future fibers) in the pericentral area. HABP staining showed that HA intensely occupied the whole cell surface area, reaching the outskirts of the cell, where the staining appeared dimmer (Fig. 2). The homogeneous distribution of HA was visibly interrupted by fibronectin pre-fibrillar arrangements (Fig. 2(R1)) and formed fibronectin fibers (Fig. 2(R2)), which carved their way through the HA cushion in the direction towards the polar edges of the cell. Hence, in relation to fibronectin, HA appeared to mainly occupy the space in between fibers, although co-localization was also observed in few locations (Fig. 2).

Next, we sought to investigate if impaired fibronectin fibrillogenesis would interfere with HA presence or distribution. Fibronectin fibrillogenesis was inhibited by disrupting the Rho A pathway, responsible for the cell-contractile machinery that acts upon fibrillar adhesions.[20] Y-27632 was used to inhibit Rho kinases (ROCK) in MSCs for 24 h, using previously published protocols,[45] in the presence or absence of exogenous HA. Actin staining showed that Y-27632 treatment caused loss of defined actin filaments and cell polarity (Fig. 3A), confirming successful ROCK inhibition.[45] To quantify differences in fibrillar fibronectin, we performed multistep image processing for the isolation and quantification of fiber length (Fig. 3D(i) and (ii)). As described previously,[20,46] the successful inhibition of cellular contractility impaired fibronectin fibril formation (Fig. 3B–D), evident by the diffuse presence of fibronectin, especially at perinuclear region and by the loss of fibrillar structures. However, ROCK inhibition had no apparent effect on HA presence or distribution. Moreover, addition of exogenous HMWHA into ROCK-inhibited cultures did not rescue fibronectin fibril formation (Fig. 3B and C). Together, these results showed that impaired fibronectin fibrillogenesis did not affect HA presence or distribution and that exogenous HA supplementation was insufficient for rescuing disrupted fibronectin fibril formation.

Hyaluronic acid was required for proper fibronectin fibril formation

In order to investigate the effect of HA on fibronectin fibrillogenesis, bmMSCs were treated with an established HA synthesis inhibitor (4-methylumbelliferone, 4-MU). Previous studies have established that 4-MU concentrations of up to 0.5 mM mainly impair HA synthases, whereas above this concentration other sulfated glycosaminoglycans (GAGs), such as heparan sulfate, were also negatively affected.[47,48] In our experimental set-up, as shown in Fig. 4, a 48 h treatment with 0.5 mM 4-MU impaired fibronectin fibrillogenesis, as evident from the accumulation of granular fibronectin at perinuclear regions and visible reduction of fibrillary fibronectin structures. Nonetheless, HABP staining revealed that HA presence and distribution was not affected at this 4-MU concentration, indicating other HA-independent effects to be responsible for the reduction in fibronectin fibrillogenesis. Hence, in our hands 4-MU appeared to be unsuitable to investigate the effect of reduction of HA on fibronectin fibrillogenesis (Fig. 4).

As an alternative to 4-MU we used chromatographically purified mammalian hyaluronidase (HAse) to remove the continuously synthesized HA. The high purity of the enzyme ensured a negligible interference from other GAG-digesting enzymes. Mammalian HAse exhibits a high substrate specificity towards HA and has a very limited ability to also degrade

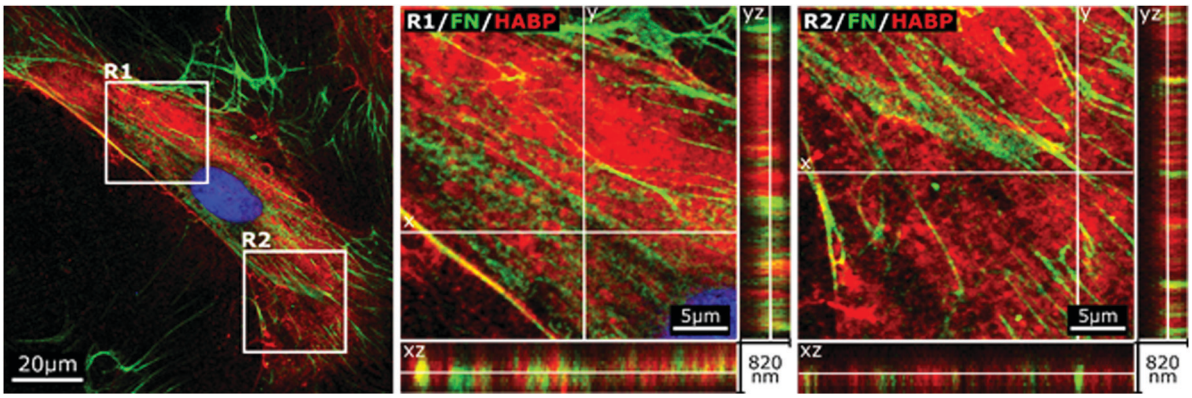

Fig. 2 Cellular HA cushions accommodate newly formed fibronectin (FN) fibers. Confocal image of immunostained FN and HABP-staining of HA in human bmMSCs on day 2. Higher magnification of orthogonal views of pre-fibrillar structures (R1) and FN fibers (R2). The selected image is representative of n = 6 biological replicates, 6500 cells per replicate.

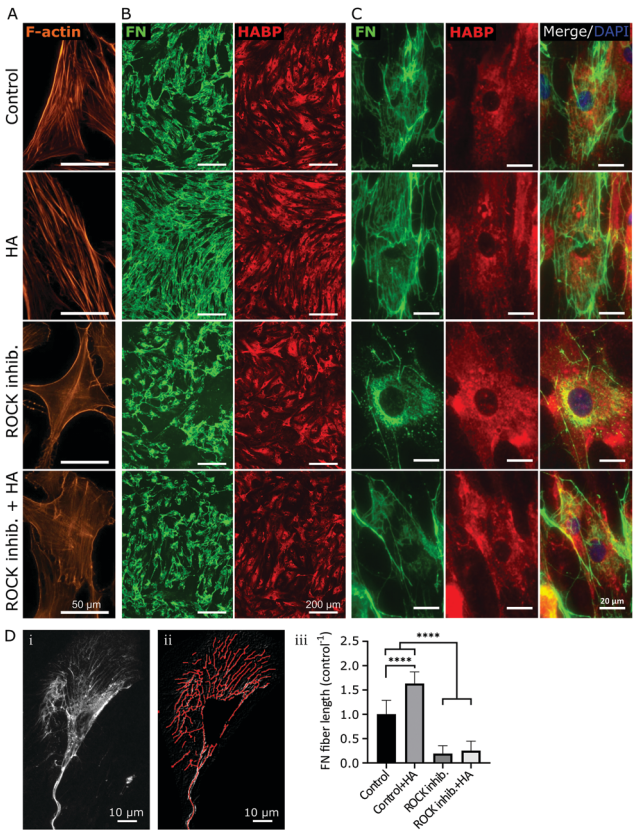

Fig. 3 Inhibition of fibronectin (FN) fibrillogenesis did not affect HA presence and distribution. Y-27632 was used to inhibit ROCK in human bmMSCs, with or without 500 µg ml^{-1} HA supplementation. Day 2 cultures were stained with phalloidin filamentous actin (F-actin) to determine effective ROCK inhibition, as confirmed by lack of organized cytoskeleton (A). Immunostained FN and HABP-staining of HA were visualized at 4× magnification (B) and 40× magnification (C) to obtain an overview over the distribution of FN and HA, as well as their cellular organization, respectively. Upon ROCK inhibition, few FN fibers were visible, and only a diffuse cellular distribution of FN was observed, whereas HA distribution was not affected. n = 6 biological replicates. Scale bar: (A) 50 µm, (B) 200 µm and (C) 20 µm. (D) Quantification of fiber length by processing acquired images (i) with ImageJ software using (ii) a fiber detection plug-in. The results are plotted as total fiber length per cell, normalized to untreated controls (iii). ****$p < 0.0001$. Scale bar: 10 µm.

chondroitin sulfate, albeit at a much slower rate and only for chondroitin sulfates with specific sulfation patterns.[49] Since chondroitin sulfates have a very low abundance in undifferentiated MSC-derived ECM,[50] we considered any interference due to potential degradation of chondroitin sulfate in our experimental set-up to be insignificant. As bmMSCs assemble ECM *in vitro* at neutral pH and HAse is most effective at acidic pH, concentrations of HA $\geq$10 U per 5 × 10^3 cells were required to degrade the continuously synthesized HA in our cultures. Moreover, the experiment was performed under serum-free conditions to avoid any effect-masking by the abundant serum-derived fibronectin. Endogenous fibronectin and HA were stained after 24 h of incubation and imaged by widefield fluorescence microscopy. In all conditions, cells attached to the surface and deposited fibronectin. Non-treated samples (Control, no HAse) and samples that were supplemented with exogenous HMWHA (HA 500 µg ml^{-1}) exhibited numerous and well-defined fibronectin fibers and a homogenous HA distribution over the entire cell body (Fig. 5A), consistent with what we observed earlier (Fig. 2 and 3). HAse treatment resulted in a detectable decrease in HA staining intensity, confirming progressive HA ablation, although low amounts of HA were still detectable (Fig. 5A). Under this partial HA depletion, significantly fewer fibronectin fibers were visible, exhibiting a diffuse and thinner appearance than in control cultures. Additionally, an intense staining of granular fibronectin was observed in the pericentral region, whereas in the periphery fibronectin staining exhibited a finely grained appearance, indicating absence of the typical fiber organization (Fig. 5A). In particular, the accumulation of granular fibronectin in the perinuclear region exhibited a high similarity to the fibronectin distribution for cells under ROCK inhibition (Fig. 3C and 5B).

Quantification of total fiber length per cell revealed a 50% decrease in the amount of fibrillar fibronectin in HAse treated cultures, as compared to untreated controls. It is noteworthy that supplementation of exogenous HA resulted in a 3-fold increase in fibronectin fibers (Fig. 5C), further confirming the data presented in Fig. 1. Together, these data showed that HA was required for fibronectin fibrillogenesis.

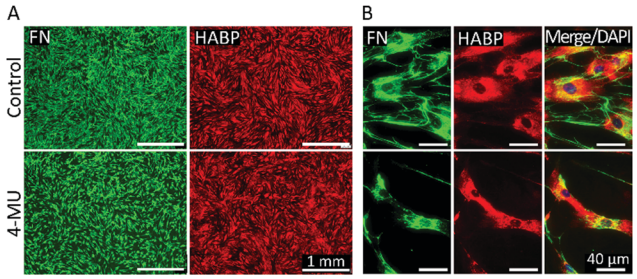

Fig. 4 4-MU disturbs fibronectin (FN) deposition and cell morphology but does not inhibit HA synthesis. bmMSCs treated with 0.5 mM 4-MU, or its vehicle, for 2 days were labelled with anti-FN and HABP for HA. (A) Low magnification micrographs show a reduction in FN covered area but not in HA presence or distribution. (B) High magnification micrographs highlight impaired FN assembly and smaller cells. Scale bar: (A) 1 mm and (B) 40 µm. n = 6 biological replicates.

In order to investigate if addition or depletion of HA might have had an effect on the expression of relevant proteins, RT-PCR was performed on samples exposed to HAse or supplemented with exogenous HMWHA. Depletion of HA had no effect on the

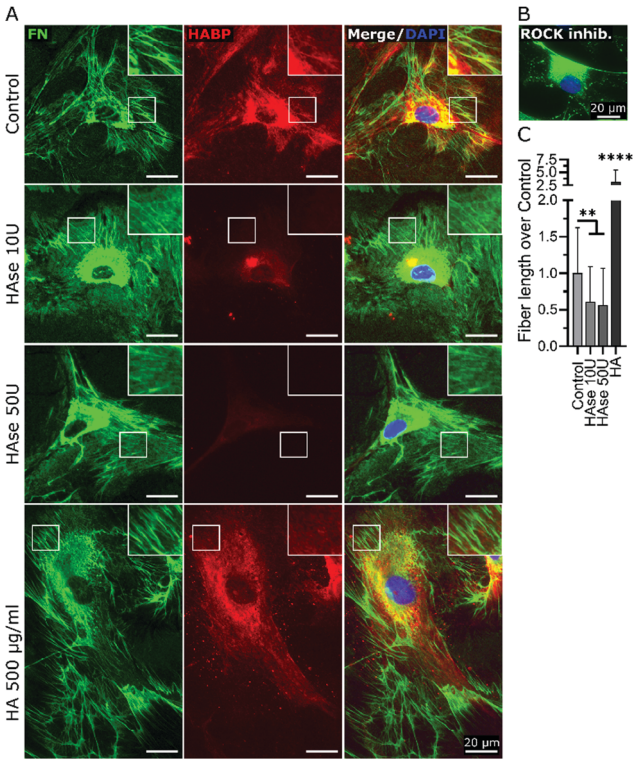

Fig. 5 HA was required for proper fibronectin (FN) fibrillogenesis. (A) Human bmMSCs were cultured in the absence of serum for 24 h, and optionally supplemented with 10 U, 50 U of HAse or 500 µg ml^{-1} HA. Respective samples were stained with anti-FN antibodies and HABP and imaged by widefield fluorescence microscopy. Nuclei were counter-stained with DAPI. Squares depict areas of higher magnification of the definition of the FN fibers (square = 18 × 18 µm). (B) Immunostained FN of a cell under ROCK-inhibition by Y-27632. (C) Quantification of fiber length by processing acquired images, plotted as total fiber length per cell normalized to untreated controls. **$p < 0.01$, ****$p < 0.0001$.

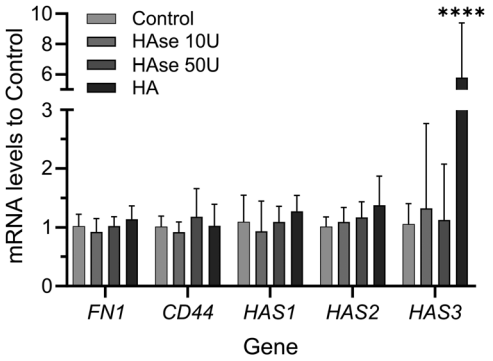

Fig. 6 Addition or depletion of HA does not affect the expression of fibronectin (FN), CD44 and the majority of HA synthases. Human bmMSCs were cultured in the absence of serum for 24 h with optional supplementation of HAse (10 U, 50 U) or HA at 500 µg ml^{-1}. Total mRNA was isolated and the levels of *FN*, *CD44*, *HAS1*, *HAS2* and *HAS3* mRNA were quantified by qRT-PCR. mRNA levels normalized to non-treated samples (control) are shown. *GAPDH* (housekeeping gene) was used to normalize individual gene expression. n = 3 biological replicates.

expression of fibronectin (*FN1*) or HA-synthase genes (mainly *HAS1*, *HAS2*, *HAS3*), or HA receptor *CD44*. Similarly, addition of exogenous HMWHA did not affect expression of *FN1*, *CD44*, *HAS1*, *HAS2*, but did significantly increase the expression of *HAS3* (Fig. 6). Thus, HA levels do not dramatically affect synthesis of fibronectin and the majority of genes associated with fibronectin fibrillogenesis.

HA was localized at sites of active fibronectin fibrillogenesis

To further elucidate the potential role of HA in the fibronectin fibrillogenesis process, we sought to investigate if HA would be localized at sites of active fibronectin fibrillogenesis. This was carried by co-staining of HA, CD44 and molecules involved in fibronectin fiber formation.

While fibronectin can be associated with both focal and fibrillar adhesions, it is the latter that exerts the necessary physical force to unfold globular fibronectin, an essential step in fibronectin fibrillogenesis.[25] Fibronectin and HA were co-stained with integrin α5, an essential factor located at the active sites of fibronectin fibrillogenesis (fibrillar adhesions), and with integrin αV, a constituent of focal adhesions, which can both recruit fibronectin dimers and bind mature fibronectin fibers.[26,51] Comparable to HA distribution, integrin α5 was found more concentrated in the pericentral cellular region and at the nucleus (Fig. 7A and Fig. S1, ESI†), where it is known to be recycled.[26] In addition, integrin α5 also associated with fibronectin fibers at all stages of maturation. Sites of fibronectin fiber formation were identified both at the sites of cell retraction (Fig. 7A) and perinuclear region (Fig. 7B), where thin fibronectin fibers in the cellular periphery, directed towards the center of the cell, transited into a discontinuous, but aligned arrangement of fibronectin molecules. Since HA, CD44, FN and integrin α5 were very abundant and not restricted to sites of fibronectin fibrillogenesis a broader view of their alignment at the sites of interest were challenging. Instead, these sites were highlighted in the regions of interest (ROIs) (Fig. 7). At these sites of active

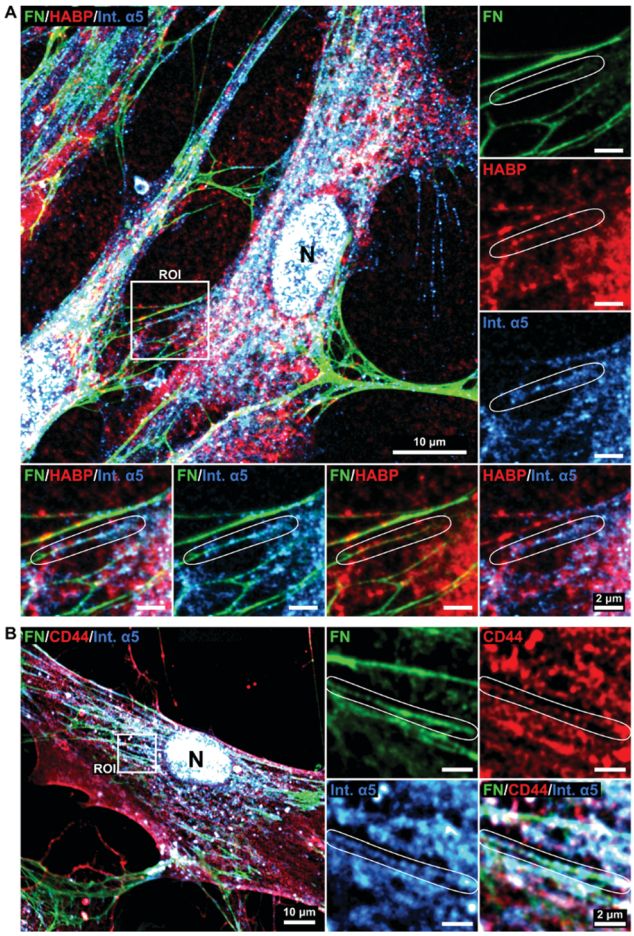

Fig. 7 HA is associated with forming fibronectin fibrils. Day 2 cultures of human bmMSCs were stained with anti-fibronectin (FN), -CD44, and -integrin α5 (int. α5) antibodies and HABP. Representative images acquired by confocal microscopy. Squares indicate regions of interest (ROIs) that are magnified at the side and depict integrin α5 at sites of active FN fibrillogenesis (fibrillar adhesions, indicated in circled areas) and HA (A) or CD44 (B). N, nucleus (DAPI stained). n = 6 biological replicates. Scale bar: 10 μm, ROIs = 2 μm.

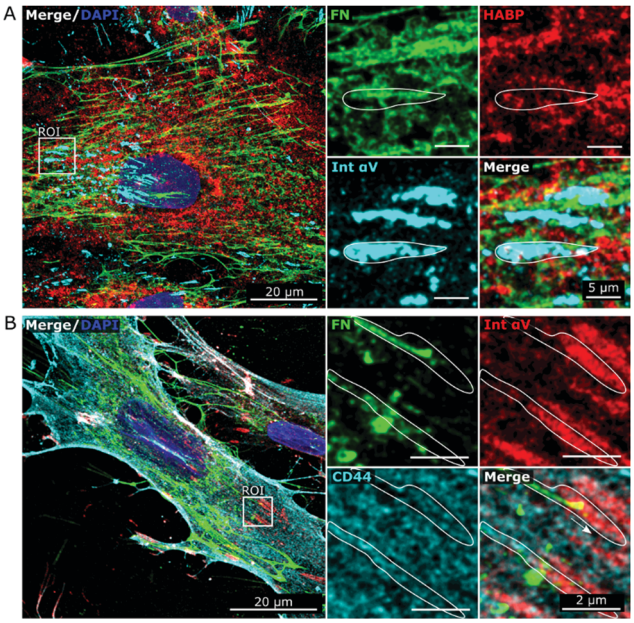

Fig. 8 Fibronectin-HA pre-fibrillar structures are not associated with focal adhesions. Human bmMSCs were cultured for 2 days and confocal images were acquired from immunostained fibronectin (FN), integrin αV (int. αV), and CD44, and HABP-labeled HA. Squares indicate regions of interest (ROIs) that are magnified at the side and depict focal adhesions (indicated by circled areas). Nuclei were counterstained with DAPI. n = 6 biological replicates. Scale bar = 20 μm, ROIs = 2 μm.

fibronectin fibrillogenesis, integrin α5 and HA co-localized with the forming fibers in a linear pattern, connecting or overlapping aligned fibronectin molecules, structurally defined as fibrillary adhesions.[52] It is noteworthy that the majority of HA and integrin α5 staining did not overlap. The tips of the forming fibronectin fibers ended in perinuclear regions, where HA and integrin α5 were highly abundant, albeit not yet assembled into a fibrillar pattern, which would have indicated fibrillar adhesions (Fig. 7A).

To further explore the relationship between HA and fibronectin we performed co-immunostainings of HA receptor CD44[53] and integrin α5 (Fig. 7B and Fig. S1, ESI†). The staining patterns revealed CD44 to be abundantly present on the whole cell surface, with a similar distribution as observed for HA (Fig. 2). Furthermore, CD44 was also found to align with integrin α5 and fibronectin in fibrillar structures (Fig. 7B).

Comparable observations were also made for MSCs supplemented with HA 500 μg ml^{-1} (Fig. S1, ESI†).

Interestingly, HA did not accumulate and did not co-localize well with focal adhesions (Fig. 8A), identified by characteristic drumstick-like clusters of integrin αV,[51] whereas CD44 was uniformly distributed in and around focal adhesions (Fig. 8B). Hence, HA appeared present at sites of active fibronectin fibrillogenesis and thus might be directly involved in the process.

Discussion

A number of HA-based biomaterials have previously been developed to promote tissue healing and regeneration, in view of the important role of HA in these processes. We observed in bmMSC cultures that supplementation with exogenous HA promoted fibronectin fibrillogenesis, measured by the increase of deposited fibrillar fibronectin. On the contrary, the partial enzyme-based depletion of endogenous HA significantly impaired fibronectin fiber formation, showing that HA is necessary for effective fibrillogenesis. Additionally, the fibronectin profile upon HA digestion (appearance, organization and localization) closely resembled that of cells with inhibited fibronectin fibrillogenesis (by means of ROCK-inhibition)[45] further confirming our hypothesis.

It should be pointed out that endogenous and exogenous HA have to be distinguished, as the former is cell-synthesized and thus often bound to the cellular surface,[54] whereas the latter is of a specific molecular weight, added to cell culture and thus freely diffusible. The difference in HA presentation could

therefore result in distinct effects in cellular responses,[55] although this was not evident in our study.

Interestingly, previous reports on the effect of HA on fibronectin deposition are controversial. In contrast to our findings, in an *in vitro* study on lung fibrosis, Evanko *et al.* reported that the disruption of HA promoted fibronectin deposition, as quantified by an increase in area coverage.[36] However, the authors made no distinction between fibrillar and non-fibrillar fibronectin. As shown in our results, even when fibronectin fibrillogenesis is completely impaired *via* ROCK-inhibition, fibronectin is still present and continues to be associated with the cell body, but lacking fibrillar structures. Indeed, in the representative pictures, depicted in the study of Evanko *et al.*, the fibrillar structure of fibronectin was lost in the absence of HA,[36] comparable to our own observations.

It is noteworthy that in an independent study, low molecular weight HA was reported to not affect fibronectin deposition,[37] indicating that HA size might be a determining factor in this process.

In accordance with our findings, HA was shown to promote fibronectin deposition *vivo*.[35] Furthermore, Shendi and co-workers observed enhanced fibronectin deposition upon addition of exogenous HA into fibroblast cultures.[33] Although their finding did not exhibit statistical significance at the experimental time-points chosen, the deposition of collagen type I was significantly increased. As fibronectin is an early deposited molecule, later time points (day 3, 7, 14) might have not been able to capture this event very well. The observed effect was claimed to be induced by the biophysical principle of macromolecular crowding (MMC).[33] Contrary to their findings, our results showed that although HA enhanced deposition of fibrillar fibronectin, collagen type I deposition was not significantly affected, even when its deposition was most obvious. Given the different observations made by us and Shendi *et al.*[33] on the effects of exogenous HA on collagen type I deposition and since we provided lower concentrations of HA, it is unlikely that MMC affected fibronectin fibrillogenesis in our experimental set-up. Since macromolecules involved in MMC are supposed to be rather inert, while excluding free volume,[16] whereas HA is known to interact with the cellular surface and various extracellular molecules,[56] other mechanisms are indeed probable to be responsible for the observed effect.

The alignment of our results with that of others provides further proof that the conclusions made based on bmMSC cultures can be extrapolated to other stromal cell types such as myofibroblasts[36] and fibroblasts,[33] as well as to *in vivo* studies.[35] It can be thus concluded that HA promotes fibronectin fibrillogenesis.

To explore the potential mechanism HA might have in the fibronectin fibrillogenesis process, we investigated the effect of HA addition or depletion on mRNA levels of fibronectin, CD44 and HA synthases. Indeed, the amount of fibronectin being synthesized appeared not to be affected, when fibrillogenesis was enhanced or impaired *via* HA addition or partial depletion, respectively. This indicates that the observed effects on the fibrillogenesis process did not depend on the amount of fibronectin being synthesized but rather point towards other HA-guided mechanisms. Of course, the expression of other genes involved in the fibrillogenesis process, and not tested here, might have been affected instead.

Our results also showed that the expression of *CD44* and *HASs* was not affected, except for *HAS3*, which was increased after supplementation of exogenous HMWHA. In a different study, increase in *HAS3* expression was observed in leading regenerative processes in the zebrafish tail,[57] pointing to additional potential mechanisms by which HA-based biomaterials might promote tissue healing and regeneration.

A potential alternative mechanism might be the direct involvement of HA in fibrillar adhesions. As indicated by our results following ROCK inhibition, which led to the expected inhibition of fibronectin fibrillogenesis, but was not accompanied by changes in HA cellular organization, HA's involvement in the firbillogenesis process might be independent of the cellular contractile apparatus.

Using integrin α5 as a visual marker for fibrillar adhesions and thus areas of fibronectin fibrillogenesis, we observed that HA and CD44 not only were connected to fibronectin but also formed linear arrangements in the direction of forming fibronectin fibers. In contrast, HA and fibronectin were less frequently observed in focal adhesions, as compared to adjacent areas. This observation suggests that such distinct alignments of HA, fibronectin molecules and integrins, as observed at fibrillar adhesions, were not transversal to all fibronectin-associated adhesions but seemed rather specific for sites of ongoing fibrillogenesis.

Based on the fact that HA has binding sites for fibronectin[27,28] and our observed spatial co-arrangement of fibronectin and HA in fibrillar adhesions, HA might indeed have a potential role in the spatial organization of fibronectin molecules. HA might promote fibronectin molecules aggregation, or even facilitate globular fibronectin unfolding. Alternatively, the high abundance, albeit not overlapping, of integrin α5 and HA in areas adjacent to the forming fibronectin fibers, might suggest HA to be involved in the spatial organization of integrin α5 into future fibrillar adhesions.

Hence, our current data indicate that HA might be directly involved in the fibronectin fibrillogenesis process. Nonetheless, other alternative mechanisms, such as the effect of HA on the cellular contractile apparatus, and the exact role of HA in fibrillar adhesions remains to be elucidated.

Conclusions

Our findings provide insights into the significant role of HA in FN fibrillogenesis. Since fibronectin is essential for ECM assembly and tissue build-up,[18,19] our findings implicate a direct mechanism through which HA guides ECM deposition.

This conclusion is of biological relevance as HA not only contributes to the first-order provisional wound matrix,[9] but also plays a pivotal role in the formation of the second order

provisional matrix.[15,17] This property of HA strongly suggests the utility of incorporating HA into biomaterials that are intended for *de novo* ECM-rich tissue formation *in vivo* and *in vitro*. Such biomaterials would be invaluable for the repair of large tissue defects, where a significant amount of tissue including ECM has to be replaced, and for engineering of tissues *in vitro*, where the assembly of an *in vivo*-like ECM-rich microenvironment is needed.[58]

The novel role of HA in ECM assembly shown here is a heretofore unknown fundamental molecular function of HA, which is essential for wound healing and tissue formation and has strong implications for the design of biomaterial-based regenerative therapies.[59]

Materials and methods

Materials

HA with molecular weights (M_r) between 1.5 and 1.8 MDa, commonly used for cell culture, was obtained from Sigma-Aldrich (Steinheim, Germany; cat# 53747, purity of 99.9%). Growth medium and supplements were obtained from Gibco (Life Technologies, Grand Island, NY, USA).

The following reagents were used to label human cultures and proteins (Table 1):

Reagents and instruments for electrophoresis and western blots were purchased from Invitrogen (Life Technologies, Rockford, IL, USA). For the cell proliferation assay, we used Cell Counting Kit-8 (Sigma Aldrich, St. Louis, MO, USA, #96992) according to the manufacturer's instructions. Absorbance at 450 nm was read in a spectrometer (Thermo Scientific Multiskan Go, Finland).

Table 1 Antibodies and reagents for immunostaining

Reagents	Host	Dilution used	Catalog #	Supplier
Primary antibodies				
Anti-fibronectin	Rabbit	1 : 500 (IF) 1 : 6000 (WB)	ab2413	Abcam
Anti-CD44	Rat	1 : 100	ab119348	Abcam
Anti-integrin α5	Mouse	1 : 150	ab78614	Abcam
Anti-collagen I	Mouse	1 : 1000	C2456	Sigma
Anti-integrin αV	Mouse	1 : 150	ab16821	Abcam
Anti-GAPDH	Rabbit	1 : 6000	ab181602	Abcam
Secondary antibodies				
Anti-rabbit AF 488		1 : 500	ab150077	Abcam
Anti-rat AF 594		1 : 500	ab150160	Abcam
Anti-mouse AF 555		1 : 500	ab150178	Abcam
Anti-mouse AF 647		1 : 1000	A31571	Molecular Probes
Anti-rabbit-HRP		1 : 5000	A27036	Molecular Probes
Others				
HABP-biotin		1 : 200	BC41	Hokudo Co.
Phalloidin-AF 555		1 : 1000	ab176756	Abcam
Streptavidin-DyLight 650		1 : 500	ab134341	Abcam
DAPI		1 : 1000	564907	BD Pharmingen

IF – immunofluorescence; WB – western blot; Suppliers: Abcam, Hong Kong; Molecular Probes, Eugene, OR, USA; Hokudo Co., Sapporo, Japan; BD Pharmingen, San Diego, CA, USA; Sigma, Saint Louis, MI, USA.

Cell culture

Human bmMSCs derived from three different donors with ages below 37 years old (Lonza, Walkersville, MD, USA; and Millipore, Temecula, CA, USA) were cultured individually to subconfluency in gelatin coated flasks with growth medium (Dulbecco's Modified Eagle's Medium (DMEM) with 1 g L^{-1} glucose and GlutaMAX, and supplemented with 10% fetal bovine serum (FBS) and 100 U ml^{-1} penicillin and 100 μg ml^{-1} streptomycin (P/S)) at 37 °C in 5% CO_2. bmMSCs were then trypsinized with TrypLE (Gibco) and seeded between passages 6 and 9 at 6.5×10^3 cells per cm^2 in tissue culture treated 48-well plates for low magnification imaging or on 8 mm diameter glass coverslips (incubated with DMEM with 10% FBS for 4 h prior seeding) for high magnification images. The cells were allowed to attach for 24 h in DMEM with 10% FBS, after which the medium was exchanged for either control medium (0.5% FBS, 0.1 mM ascorbic acid; Sigma-Aldrich, #A8960) or HA containing medium (5, 50, 500 or 1000 μg ml^{-1} HMWHA and 0.5% FBS, 0.1 mM ascorbic acid). The bmMSCs were processed for cytochemistry 2 days post-induction.

Inhibition and degradation assays

For the inhibition of Rho kinases 1 and 2 (ROCK 1/2) in bmMSCs, cells were treated 24 h after cell seeding with the inhibitor Y-27632 (StemCell technologies, Vancouver, Canada, #72302), as previously decribed.[45] Briefly, Y-27632 was added to culture medium at 10 μM for 24 h.

HA synthesis inhibition was performed according to the method of Kultti *et al.*[48] using 4-MU. Briefly, cultures were treated for 24 h with 4-MU (Sigma-Aldrich, #M1381) at 0.5 mM in the medium.

For titrated HA digestion, the cells were cultured in the absence of FBS to avoid any effect-masking by the abundant serum-derived fibronectin and treated with chromatographically purified mammalian HAse (Worthington, Lakewood, NJ, USA, #LS005477) at enzyme concentrations above 10 U per 5.0×10^3 cells for 24 h. The perturbation experiments were carried out in the presence or absence of HMWHA 500 μg ml^{-1}. Controls consisted of supplementation of delivery vehicles (PBS for ROCK and HAse; 0.1% dimethyl sulfoxide for 4-MU). All cultures were fixed with methanol for subsequent analysis.

Removal of non-fibrillar fibronectin

Non-fibrillar fibronectin was extracted from the cell layers following the procedure of Sechler *et al.*[41] Briefly, bmMSCs cultures prepared as described above were washed twice with phosphate-buffered saline (PBS) and incubated for 10 min with ice cold DOC, 0.25% (w/v) in water; Sigma-Aldrich, Steinheim, Germany, #30970. The remaining ECM was washed with ice cold PBS for 15 min and fixed for 15 min with ice cold methanol.

Cytochemistry

For staining of fibronectin or HA alone, methanol-fixation was used, whereas in experiments requiring actin and integrin staining, paraformaldehyde (PFA) fixation was used. Briefly, the

cell layers were washed with PBS, fixed for 10 min with ice cold methanol or for 20 min with 4% PFA (Thermo Scientific), and then permeabilized with 0.5% saponin (Riedel-de Haën, Seelze, Germany, #70940) for 10 min. Subsequently, after blocking for 1 h with 3% bovine serum albumin (BSA, Sigma-Aldrich, #A7906; in 0.1% saponin–PBS for PFA-fixed samples), the cultures were first incubated overnight at 4 °C with the primary antibodies and HABP in 1% BSA (and 0.1% saponin for PFA-fixed samples), washed, and then followed by secondary antibodies or other dyes (such as DAPI and phalloidin) for 2 h at room temperature. Finally, the samples were washed with PBS mounted in Prolong Glass (Invitrogen, Life Technologies, Eugene, Oregon, USA; #P36984), and visualized.

Real time reverse transcription-PCR

Total RNA was isolated from cell cultures with RNAiso plus (TAKARA, Shiga, Japan, cat#:9109). mRNA was reverse transcribed into cDNA using PrimeScript RT Master Mix (TaKaRa, Shiga, Japan, Cat#: RR036A). Real time PCR (qPCR) was done using ABI QuantStudio7 Flex Real Time PCR System (Applied Biosystems, Carlsbad, CA) with TB Green Premix Ex Taq (TaKaRa, Shiga, Japan, Cat#: RR420A). cDNA was amplified using the following human gene primers (Table 2):

The cycle thresholds (Ct) were normalized to *GAPDH* and ΔΔCt was calculated in relation to control. To validate that *GAPDH* expression was not affected by culture conditions, *B2M* was also used as an alternative housekeeping gene, which yielded similar results.

Microscopy

Epifluorescence images were taken with an Olympus IX83 inverted fluorescence microscope (Olympus, Tokyo, Japan) equipped with CellSense Dimension image acquisition software (Olympus, Tokyo, Japan). Fibronectin covered area were image-acquired using a 4× objective, where each image represented 14 mm^2, 15% of total well area. The images were processed and quantified using NIH Image J v1.52i software (https://imagej.nih.gov/ij/) by excluding the background *via* threshold setting and applying a binary mask.

Table 2 RT-PCR gene primer sequences

Gene	Sequence (5′ → 3′)
FN1	F: GTAGGGGTCAAAGCACGAGTCATC
	R: GTCCCGGTGAGACAGATGAG
HAS1	F: CTACTGGGTGGCCATGTTGA
	R: ACCACCCAGCAAGTTCGTG
HAS2	F: GTCCCGGTGAGACAGATGAG
	R: AGGCTGGGTCAAGCATAGTG
HAS3	F: ATCCCCAAGTAGGGGGAGTC
	R: AACCAGCAGGGAGTTAGCAC
CD44	F: GGGTCCCATACCACTCATGG
	R: TTCTGCCCACACCTTCTTCG
GAPDH	F: CCAGGGCTGCTTTTAACTCTGGTAAAGTGG
	R: ATTTCCATTGATGACAAGCTTCCCGTTCTC
B2M	F: CCGTGTGAACCATGTGACTT
	R: CCAATCCAAATGCGGCATCT

Abbreviations: F, forward; R, reverse; *GAPDH*, glyceraldehyde 3-phosphate dehydrogenase; *B2M*, β2 microglobulin.

Confocal images were acquired using a Leica TCS SP8 inverted microscope equipped with HyD and PMT detectors, using Pulse laser source (WLL) and a 63× oil-immersion objective (Leica Microsystems, Wetzlar, Alemanha). The images were acquired with LASX SP8 software (Leica Microsystems, Wetzlar, Alemanha) in Lightning mode with 4 scan sequences, one for each channel, to prevent crosstalk. Line bi-directional scanning was the imaging mode used to prevent displacement in between channels.

Fiber quantification

Fibronectin images acquired with a 40× objective and a wide-field microscope were processed using NIH Image J v1.52p by (1) isolating each cell, (2) subtracting background with constant ball radius per each run, (3) manually removing the non-fibrillar fibronectin cell core, and (4) executing Ridge Detection plug-in (σ = 1.4, minimum fiber size = 8 pixels, lower threshold = 3.4). The resulting fiber data points of each cell, and their lengths, were summed and normalized over the average sum of the respective control.

Statistical analysis

Statistical analysis on cytochemistry data was performed with One- or Two-way Analysis of Variance algorithm after confirming that the assumptions of normality and equal variance were met. The summarized results were obtained from at least three independent biological runs, each containing at least 3 replicates. *Post hoc* Tukey tests were used for multi-comparison, and p-values <0.05 were considered statistically significant. All analyses were performed using GraphPad Prism v8.0 (GraphPad Software, San Diego, CA, USA, www.graphpad.com).

Author contributions

MA performed most of the experimentation, image processing, data computation and analysis. CHKY assisted with ROCK inhibition and HAse inhibition experiments and image processing. HYW performed PCR analysis. AB conceived the study and performed part of the experiments and data analysis. MA and AB interpreted data and wrote the manuscript. DW, DFEK and RST contributed to data interpretation and edited the manuscript.

Conflicts of interest

There are no conflicts to declare.

Acknowledgements

MA would like to acknowledge the Institute for Tissue Engineering and Regenerative Medicine and the School of Biomedical Sciences, CUHK, for her post-graduate scholarship. All authors appreciate the support from the School of Biomedical Sciences core facilities, and would like to specifically thank Josie Lai, Anny Cheung and Venus Yeung for their technical knowledge and support. Funding support include a

laboratory start-up grant (8508266) from CUHK (AB), a direct grant (2019.016) from the Faculty of Medicine, CUHK (AB), a grant by the Innovation and Technology Commission of Hong Kong, SAR (ITS/116/19; AB), and the Lee Quo Wei and Lee Yick Hoi Lun Professorship in Tissue Engineering and Regenerative Medicine (RST).

References

1 R. C. Gupta, R. Lall, A. Srivastava and A. Sinha, *Front. Vet. Sci.*, 2019, **6**, 192.
2 L. H. Chen, J. F. Xue, Z. Y. Zheng, M. Shuhaidi, H. E. Thu and Z. Hussain, *Int. J. Biol. Macromol.*, 2018, **116**, 572–584.
3 Z. Hussain, H. E. Thu, H. Katas and S. N. A. Bukhari, *Polym. Rev.*, 2017, **57**, 594–630.
4 Y. P. Singh, J. C. Moses, N. Bhardwaj and B. B. Mandal, *J. Mater. Chem. B*, 2018, **6**, 5499–5529.
5 A. R. Short, D. Koralla, A. Deshmukh, B. Wissel, B. Stocker, M. Calhoun, D. Dean and J. O. Winter, *J. Mater. Chem. B*, 2015, **3**, 7818–7830.
6 S. Amorim, C. A. Reis, R. L. Reis and R. A. Pires, *Trends Biotechnol.*, 2021, **39**, 90–104.
7 Y. Xin, P. Xu, X. Wang, Y. Chen, Z. Zhang and Y. Zhang, *Stem Cell Res. Ther.*, 2021, **12**, 49.
8 M. A. Missinato, K. Tobita, N. Romano, J. A. Carroll and M. Tsang, *Cardiovasc. Res.*, 2015, **107**, 487–498.
9 K. L. Aya and R. Stern, *Wound Repair Regen.*, 2014, **22**, 579–593.
10 D. Chester and A. C. Brown, *Matrix Biol.*, 2017, **60–61**, 124–140.
11 J. S. Frenkel, *Int. Wound J.*, 2014, **11**, 159–163.
12 P. L. Bollyky, B. A. Falk, S. A. Long, A. Preisinger, K. R. Braun, R. P. Wu, S. P. Evanko, J. H. Buckner, T. N. Wight and G. T. Nepom, *J. Immunol.*, 2009, **183**, 2232–2241.
13 D. Jiang, J. Liang and P. W. Noble, *Physiol. Rev.*, 2011, **91**, 221–264.
14 Z. Julier, A. J. Park, P. S. Briquez and M. M. Martino, *Acta Biomater.*, 2017, **53**, 13–28.
15 X. M. Ang, M. H. C. Lee, A. Blocki, C. Chen, L. L. S. Ong, H. H. Asada, A. Sheppard and M. Raghunath, *Tissue Eng., Part A*, 2014, **20**, 966–981.
16 C. Chen, F. Loe, A. Blocki, Y. Peng and M. Raghunath, *Adv. Drug Delivery Rev.*, 2011, **63**, 277–290.
17 T. H. Barker and A. J. Engler, *Matrix Biol.*, 2017, **60–61**, 1–4.
18 R. Kinsey, M. R. Williamson, S. Chaudhry, K. T. Mellody, A. McGovern, S. Takahashi, C. A. Shuttleworth and C. M. Kielty, *J. Cell Sci.*, 2008, **121**, 2696–2704.
19 I. Valiente-Alandi, S. J. Potter, A. M. Salvador, A. E. Schafer, T. Schips, F. Carrillo-Salinas, A. M. Gibson, M. L. Nieman, C. Perkins, M. A. Sargent, J. Huo, J. N. Lorenz, T. DeFalco, J. D. Molkentin, P. Alcaide and B. C. Blaxall, *Circulation*, 2018, **138**, 1236–1252.
20 C. Zhong, M. Chrzanowska-Wodnicka, J. Brown, A. Shaub, A. M. Belkin and K. Burridge, *J. Cell Biol.*, 1998, **141**, 539–551.
21 R. Pankov, E. Cukierman, B. Z. Katz, K. Matsumoto, D. C. Lin, S. Lin, C. Hahn and K. M. Yamada, *J. Cell Biol.*, 2000, **148**, 1075–1090.
22 S. Huveneers, H. Truong, R. Fassler, A. Sonnenberg and E. H. J. Danen, *J. Cell Sci.*, 2008, **121**, 2452–2462.
23 C. A. Lemmon and S. H. Weinberg, *Sci. Rep.*, 2017, **7**, 18061.
24 J. E. Schwarzbauer, *J. Cell Biol.*, 1991, **113**, 1463–1473.
25 V. Schaufler, H. Czichos-Medda, V. Hirschfeld-Warnecken, S. Neubauer, F. Rechenmacher, R. Medda, H. Kessler, B. Geiger, J. P. Spatz and E. A. Cavalcanti-Adam, *Cell Adhes. Migr.*, 2016, **10**, 505–515.
26 E. Rainero, J. D. Howe, P. T. Caswell, N. B. Jamieson, K. Anderson, D. R. Critchley, L. Machesky and J. C. Norman, *Cell Rep.*, 2015, **10**, 398–413.
27 M. Nakamura, H. Mishima, T. Nishida and T. Otori, *J. Cell. Physiol.*, 1994, **159**, 415–422.
28 K. M. Yamada, D. W. Kennedy, K. Kimata and R. M. Pratt, *J. Biol. Chem.*, 1980, **255**, 6055–6063.
29 D. A. Frenz, S. K. Akiyama, D. F. Paulsen and S. A. Newman, *Dev. Biol.*, 1989, **136**, 87–96.
30 J. Govindan and M. K. Iovine, *Gene Expression Patterns*, 2015, **19**, 21–29.
31 M. Dobaczewski, M. Bujak, P. Zymek, G. Ren, M. L. Entman and N. G. Frangogiannis, *Cell Tissue Res.*, 2006, **324**, 475–488.
32 S. E. Mercer, S. J. Odelberg and H.-G. Simon, *Dev. Biol.*, 2013, **382**, 457–469.
33 D. Shendi, J. Marzi, W. Linthicum, A. J. Rickards, D. M. Dolivo, S. Keller, M. A. Kauss, Q. Wen, T. C. McDevitt, T. Dominko, K. Schenke-Layland and M. W. Rolle, *Acta Biomater.*, 2019, **100**, 292–305.
34 M. A. Mariggiò, A. Cassano, A. Vinella, A. Vincenti, R. Fumarulo, L. Lo Muzio, E. Maiorano, D. Ribatti and G. Favia, *Int. J. Immunopathol. Pharmacol.*, 2009, **22**, 485–492.
35 J. Gaston and S. L. Thibeault, *Biomatter*, 2013, **3**, e23799.
36 S. P. Evanko, S. Potter-Perigo, L. J. Petty, G. A. Workman and T. N. Wight, *Matrix Biol.*, 2015, **42**, 74–92.
37 S. Vogel, S. Arnoldini, S. Möller, M. Schnabelrauch and U. Hempel, *Sci. Rep.*, 2016, **6**, 1–13.
38 R. K. Schneider, J. Anraths, R. Kramann, J. Bornemann, M. Bovi, R. Knüchel and S. Neuss, *Biomaterials*, 2010, **31**, 7948–7959.
39 F. R. Maia, K. B. Fonseca, G. Rodrigues, P. L. Granja and C. C. Barrias, *Acta Biomater.*, 2014, **10**, 3197–3208.
40 A. Blocki, S. Beyer, J.-Y. Dewavrin, A. Goralczyk, Y. Wang, P. Peh, M. Ng, S. S. Moonshi, S. Vuddagiri, M. Raghunath, E. C. Martinez and K. K. Bhakoo, *Biomaterials*, 2015, **53**, 12–24.
41 J. L. Sechler, Y. Takada and J. E. Schwarzbauer, *J. Cell Biol.*, 1996, **134**, 573–583.
42 C. Chen, F. Loe, A. Blocki, Y. Peng and M. Raghunath, *Adv. Drug Delivery Rev.*, 2011, **63**, 277–290.
43 M. Assunção, C. W. Wong, J. J. Richardson, R. Tsang, S. Beyer, M. Raghunath and A. Blocki, *Mater. Sci. Eng., C*, 2020, **106**, 110280.
44 J. Laterra and L. A. Culp, *J. Biol. Chem.*, 1982, **257**, 719–726.

45 M. Amano, M. Nakayama and K. Kaibuchi, *Cytoskeleton*, 2010, **67**, 545–554.
46 Q. Zhang, M. K. Magnusson and D. F. Mosher, *Mol. Biol. Cell*, 1997, **8**, 1415–1425.
47 K. Rilla, S. Pasonen-Seppänen, J. Rieppo, M. Tammi and R. Tammi, *J. Invest. Dermatol.*, 2004, **123**, 708–714.
48 A. Kultti, S. Pasonen-Seppänen, M. Jauhiainen, K. J. Rilla, R. Kärnä, E. Pyöriä, R. H. Tammi and M. I. Tammi, *Exp. Cell Res.*, 2009, **315**, 1914–1923.
49 R. Stern and M. J. Jedrzejas, *Chem. Rev.*, 2006, **106**, 818–839.
50 M. Marinkovic, O. N. Tran, T. J. Block, R. Rakian, A. O. Gonzalez, D. D. Dean, C. K. Yeh and X. D. Chen, *Matrix Biol. Plus*, 2020, **8**, 100044.
51 R. Changede, X. Xu, F. Margadant and M. P. Sheetz, *Dev. Cell*, 2015, **35**, 614–621.
52 D. M. Peters and D. F. Mosher, *J. Cell Biol.*, 1987, **104**, 121–130.
53 D. S. Bhattacharya, D. Svechkarev, J. J. Souchek, T. K. Hill, M. A. Taylor, A. Natarajan and A. M. Mohs, *J. Mater. Chem. B*, 2017, **5**, 8183–8192.
54 U. Anderegg, J. C. Simon and M. Averbeck, *Exp. Dermatol.*, 2014, **23**, 295–303.
55 D. D. Allison, K. R. Braun, T. N. Wight and K. J. Grande-Allen, *Acta Biomater.*, 2009, **5**, 1019–1026.
56 K. T. Dicker, L. A. Gurski, S. Pradhan-Bhatt, R. L. Witt, M. C. Farach-Carson and X. Jia, *Acta Biomater.*, 2014, **10**, 1558–1570.
57 X. Ouyang, N. J. Panetta, M. D. Talbott, A. Y. Payumo, C. Halluin, M. T. Longaker and J. K. Chen, *PLoS One*, 2017, **12**, e0171898.
58 M. Assunção, D. Dehghan-Baniani, C. H. K. Yiu, T. Später, S. Beyer and A. Blocki, *Front. Bioeng. Biotechnol.*, 2020, **8**, 1378.
59 S. Beyer, M. Koch, Y. H. Lee, F. Jung and A. Blocki, *Int. J. Mol. Sci.*, 2018, **19**, 2913.